The Australian Journal of Agricultural and Resource Economics

Australian Journal of Agricultural and Resource Economics, 65, pp. 66–93

Can satellite-based weather index insurance improve the hedging of yield risk of perennial non-irrigated olive trees in Spain?*

Wienand Kölle, Andrea Martínez Salgueiro, Matthias Buchholz and Oliver Musshoff†

Olive oil yields fluctuate strongly due to their dependence on sufficient precipitation. An interesting option to hedge the yield risk in olive cultivation could be satellite-based weather index insurance. Therefore, we implement index insurance as a hedging alternative for non-irrigated olive groves using MODerate-resolution Imaging Spectroradiometer (MODIS) satellite data. For this purpose, we focus on the Spanish region of Andalusia, given its importance in olive production at the international level. We calculate three satellite indices: the Vegetation Condition Index (VCI), the Temperature Condition Index (TCI) and the Vegetation Health Index (VHI). Meteorological indices related to temperature and precipitation are used as benchmarks. Firstly, we estimate the periods that have the greatest influence on the critical vegetative phase of olives, which extends from March to September. Based on the indices, insurance contracts are designed using a copula approach, which is then employed to evaluate their hedging effectiveness. On average, the hedging effectiveness of VCI-, VHI- and TCI-based weather index insurance contracts amounts to 38 per cent, 38 per cent and 29 per cent, respectively. Moreover, VCI- and VHI-based weather index insurance contracts outperform traditional weather index insurance contracts based on precipitation (by 29 per cent) and temperature (by 16 per cent) indices.

Key words: copulas, olive trees, remotely sensed data, risk management, tail dependence, weather index insurance.

1. Introduction

The effects of climate change such as droughts severely affect plantation crops (Gunathilaka *et al.* 2018a). Numerous studies investigate the effect of climate change on perennial crops such as fruit crops in the United States (Deschenes and Kolstad 2011), viticulture in Germany (Ashenfelter and Storchmann 2010) and tea in China (Boehm *et al.* 2016) and Sri Lanka (Gunathilaka *et al.*

* The project which has generated these results has been supported by a grant of Fundación Bancaria 'la Caixa' (ID 100010434), whose code is LCF/BQ/ES16/11570002. Open access funding enabled and organized by Projekt DEAL.

†Wienand Kölle (email: wienand.koelle@uni-goettingen.de) and Matthias Buchholz are Research Scholars and Oliver Musshoff is Professor with the Department of Agricultural Economics and Rural Development, Georg-August-University Göttingen, Platz der Göttinger Sieben 5, Göttingen, D-37073, Germany. Andrea Martínez Salgueiro is Research Scholar at the Department of Business, Universitat Autònoma de Barcelona (UAB), Building B, Campus UAB, Bellaterra, Cerdanyola del Vallès, Barcelona, 08193, Spain.

doi: 10.1111/1467-8489.12403

2017). In perennial cropping systems production cannot be adapted to climate change as easily as in systems with annual crops (Gunathilaka *et al.* 2018b). The high capital costs upfront, the frequent non-irrigated cultivation and the long life span of plantation crops make it difficult to adapt to climate change (Gunathilaka *et al.* 2018a).

Against this background, agricultural crop insurance offers the possibility of a reduction in weather-related production risks. Indemnity-based insurance is often used to insure against damage caused by frost, hail and drought, for example. Accordingly, the indemnity payment is based on the respective amount of damage and requires its determination, which results in relatively high administrative costs (Collier *et al.* 2009). Further challenges of indemnity-based insurance consist of problems such as moral hazard and adverse selection (Goodwin 2001). In order to avoid such problems, weather index insurance in agriculture is being increasingly investigated (Turvey 2001; Leblois *et al.* 2014; Vedenov and Barnett 2004). In contrast to common agricultural crop insurance, compensation payments of a weather index insurance are based on the level of an objectively measurable index. As a result, the indemnity payment can be derived directly from the level of the index value, in that an indemnity payment is made if a certain threshold value is undershot or exceeded (Skees *et al.* 1997). The choice of an objective index highly correlated with crop yield is an essential prerequisite for effective weather index insurance. Oftentimes, station-based weather data such as accumulated temperature and precipitation are used as underlyings for weather index insurance. As precipitation is spatially heterogeneous, the effectiveness of insurance using station-based weather data is strongly dependent on proximity to the reference weather station to reduce the basis risk - meaning an insufficient correlation between index and crop yield (Gommes and Göbel 2013). Thus, the effectiveness of station-based weather index insurance is prone to geographical basis risk (Turvey 2001; Vedenov and Barnett 2004). Due to their non-reliance on weather stations, remotely sensed indices could be an effective way of reducing the basis risk of weather index insurance (Makaudze and Miranda 2010). These indices are based on data collected by remote sensing. With remote sensing, images are generated by cameras on satellites or airplanes for the purpose of monitoring areas and detecting changes in the earth's surface. Since light is emitted or absorbed to different degrees depending on the condition of the plant or soil, remotely sensed images can be used to draw conclusions about the state of vegetation (USGS 2020). As satellite indices in particular are provided almost in real time and are available free of charge for every location worldwide (Quiring and Ganesh 2010), satellite-based weather index insurance could be of interest in countries where a dense network of weather stations is not available. In this context, Ward *et al.* (2020) propose in their study on rice smallholders in India the consideration of satellite indices for the purpose of weather index insurance.

Against the background of a challenging adaptation of plantation crops to climate change, our study considers olive trees in Andalusia. Although olive trees are well adapted to low precipitation in Andalusia, the variability of olive yields has increased over the last 20 years (Quiroga and Iglesias 2009). One possible risk management strategy is irrigation, which reduces yield losses in olive cultivation (Lavee *et al.* 1990). According to Martínez and Almonacid (2017), the area of irrigated olive groves in Andalusia will continue to increase in the future as there are no attractive alternatives to irrigation to ensure high olive yields. Therefore, without appropriate alternatives, adequate management of the scarce resource water will become more and more critical (Martínez and Almonacid 2017). Against this background, Salazar *et al.* (2019) observe that for Chilean farms the risk management tools of irrigation and insurance are used as substitutes, which creates a negative relationship between irrigation use and participation in an insurance program.

In order to avoid the problems associated with irrigation, the effect of satellite-based weather index insurance on perennial crops in plantations like olives, citrus, apples and grapevines has not yet been further investigated. For perennial crops such as olive orchards, satellite images have so far only been used to identify drought-induced vegetation stress (Shivers *et al.* 2019) and to estimate the gross primary production (Brilli *et al.* 2013). So far, satellite-based weather index insurance is offered only for grassland in Canada, Spain and France (Vroege *et al.* 2019). To close this research gap, this paper will examine satellite-based weather index insurance for non-irrigated olive trees in Andalusia. Although the study is based on olive trees in this Spanish region, the methodology and results could also be of interest for other perennial plantation crops in other areas and countries. The objective of this paper is twofold. First, we investigate in which phases of vegetation the satellite-based vegetation health indices show the greatest relationship with olive oil yields in Andalusia. Secondly, we investigate the potential of satellite-based weather index insurance for hedging the yield risk of non-irrigated olive trees. For this purpose, we also compare satellite-based and meteorological-based weather index insurance contracts in order to be able to make statements about the basis risk.

To the best of our knowledge, this is the first study to examine insurance in olive cultivation, especially weather index insurance contracts. To answer the research questions, the following remotely sensed vegetation health indices from relatively high-resolution (250 × 250 m) MODIS satellite images are calculated: the Vegetation Condition Index (VCI), the Temperature Condition Index (TCI) and the Vegetation Health Index (VHI). While the VCI describes the current state of vegetation by representing the amount of green biomass, the TCI represents the temperature conditions. In addition, the VHI is a combined index composed of the VCI and the TCI. Other studies use

satellite images with lower resolution for the design of satellite-based weather index insurance with the VCI, TCI and VHI for non-perennial crops (Bokusheva *et al*. 2016; Möllmann *et al*. 2019). Since several studies report on the influence of extreme weather conditions on olive yields (Oteros *et al*. 2013; Ozdemir 2016), we design weather index insurance contracts against extreme weather events. For this purpose we use a copula approach for a proper and robust estimation of yield dependence on extreme weather conditions. We expect that the copula approach can better explain extreme yield losses, as copulas can constitute tail dependence compared to the commonly used correlation method, which assumes a linear relationship between index and crop yield (Embrechts *et al*. 2002). The satellite-based weather index insurance refers to the respective province level in Andalusia, since the olive oil yields are not available at farm level but only at the aggregated province level. However, a precise identification of olive fields and the use of relatively high-resolution satellite data result in a very high proportion of cultivated land per pixel of the satellite images. As a result, the satellite index values are not distorted by other landscape elements such as mountains, lakes, forests, etc., as in other studies with lower resolution.

The rest of the paper is structured as follows: a brief overview of challenges in the context of weather index insurance is given in section two. Section three describes the satellite indices, whereas section four deals with the copula approach for the design of weather index insurance. Section five describes the study area and data used. After the presentation of results and discussion in sections six and seven, the paper ends with a conclusion in section eight.

2. Challenges of weather index insurance

Despite the advantages of weather index insurance over indemnity-based insurance, weather index insurance as a financial risk management alternative is still not very common in agriculture. In addition to the basis risk (Barnett and Mahul 2007), the low demand for weather index insurance could also be due to model prediction uncertainties (Bokusheva and Breustedt 2012).

In order to reduce the basis risk the use of satellite-based weather index insurance appears to be promising. Previous studies have focused mainly on the use of the Normalized Difference Vegetation Index (NDVI) for insurance purposes. The NDVI reflects photosynthetic activity, vitality and density of the plant vegetation. This index has often been suggested as an underlying for forage insurance, given its ability to measure biomass (Chantarat *et al*. 2013; Leblois *et al*. 2014; Miranda and Farrin 2012). In addition, Makaudze and Miranda (2010) show that the NDVI-based weather index insurance for maize and cotton yields can reduce basis risk compared to the commonly used precipitation-based weather index insurance. According to Turvey and Mclaurin (2012), the NDVI has some limitations as an underlying for weather

index insurance, as the NDVI does not include any necessary site calibration taking into account effects such as soil type, topography and nutrient uptake. In order to account for differences between production sites, Kogan (1995) developed the three satellite-based vegetation health indices VCI, TCI and VHI. The vegetation health indices are mainly used in the agriculture sector to predict yields and identify droughts (Kogan *et al.* 2003; Kogan *et al.* 2012; Kogan 1998; Unganai and Kogan 1998). Bokusheva *et al.* (2016) use the VCI and TCI as indices for weather index insurance and can confirm that VCI- and TCI-based insurance contracts are suitable for insuring winter wheat yield risk. In a German case study for winter wheat, Möllmann *et al.* (2019) find that weather index insurance based on the VCI, TCI and VHI is superior to weather index insurance based on meteorological indices in most cases.

However, model prediction uncertainties can also be a problem of weather index insurance. The usual methods, which assume a linear relationship between index and crop yield, have some limitations. The crop yield does not react consistently to all possible realisations of a weather variable (Schlenker and Roberts 2006). For example, plant reactions to increased precipitation depend heavily on the water supply currently available. Thus, a proper contract design is a key issue to exploit the potential of weather index insurance (Kapphan *et al.* 2012). Against this background, Bokusheva *et al.* (2016) and Möllmann *et al.* (2019) assumed that the dependence between crop yield and a weather index chosen to reflect catastrophic weather events is stronger and more stable under extreme observations. While Möllmann *et al.* (2019) apply the Quantile Regression (QR) for this purpose, Bokusheva *et al.* (2016) also use the copula approach. Consequently, a more precise representation of the dependency structure between index and crop yield leads to a better performance of index insurance. So farmers are confronted with below-average situations in case of an insured event and it is therefore relevant to include these events in insurance contracts (Conradt *et al.* 2015). Therefore, we assume that the dependence between olive oil yields and satellite indices chosen to reflect catastrophic weather events is stronger and more stable under extreme observations. As a result, we obtain more robust estimates of yield dependence on weather conditions, which considerably reduces model prediction uncertainties (Bokusheva 2018).

3. Vegetation health indices

In the analysis, we calculate the three satellite indices VCI, TCI and VHI. For the calculation of the VCI we use the Enhanced Vegetation Index (EVI)[1]. Like the NDVI, the EVI is a satellite index representing the change in green plant biomass during the vegetation period (Salem *et al.* 1995). The EVI quantifies the total amount of green biomass in each pixel of a satellite image

[1] We find higher correlations for the EVI with the olive oil yield than for the NDVI.

during a given study period. Compared to NDVI, the EVI has a higher sensitivity to regions with a high biomass. The EVI is calculated according to the following formula:

$$EVI = 2.5\left(\frac{NIR - Red}{NIR + 2.4Red + 1}\right). \quad (1)$$

The EVI has a stronger vegetation monitoring capability, because the canopy background signals and the influences of the atmosphere are diminished by the EVI calibration coefficients (Didan *et al*. 2015). The idea behind the index is that in moisture-stressed, dry vegetation, a higher reflection at the Red spectral band (Red) and a lower reflectance at near-infrared (NIR) spectral bands is present compared to normal, non-moisture-stressed vegetation, so that dryness is reflected in low EVI values (Spivak *et al*. 2008).

The VCI is calculated by normalising the EVI values using the perennial absolute minimum and maximum values. The normalisation eliminates effects of the natural site conditions (soil, topography, etc.) that affect the EVI value to varying degrees. Thus, the same EVI values must be interpreted differently depending on the ecological potential of the region. The absolute maximum and minimum EVI values of each pixel include the extreme weather conditions. Thus, those EVI values reflect the minimum or maximum limitation of the yield capacity specified by the ecosystem as reference points. Finally, the VCI indicates to what extent the respective weather conditions exploit the ecological potential of the region (Kogan 1995). The VCI is calculated by the minimum (EVI_{min}) and maximum (EVI_{max}) EVI values for each pixel of the study period and for each satellite image with the temporal resolution of r as follows:

$$VCI_r = 100 \cdot \frac{EVI_r - EVI_{min}}{EVI_{max} - EVI_{min}}. \quad (2)$$

The VCI is represented on a scale from 0 to 100 (Kogan 1995). Consequently, higher VCI values indicate vital vegetation that is not characterised by moisture stress. By contrast, dry years are characterised by a lower green biomass and correspondingly lower VCI values, which are caused by thermal vegetation stress due to drought. However, other factors, such as plant diseases or insects, can also influence the amount of green biomass, but these mainly occur as local effects, whereas drought tends to affect larger areas or regions.

In addition, the TCI is also included in the study to identify vegetation stress by taking temperature into account. The TCI determines the thermal conditions of the land surface taking into account the plant coverage (Kogan *et al*. 2012). The normalised TCI is calculated using Landsurface Temperatures (LST) values for each year and pixel of the satellite image with the temporal resolution of r as follows:

$$TCI_r = 100 \cdot \frac{LST_{max} - LST_r}{LST_{max} - LST_{min}}. \quad (3)$$

LST_{min} and LST_{max} correspond to the minimum and maximum LST values over several years (Unganai and Kogan 1998). The TCI values also range from 0 to 100. In accordance with the VCI, low values indicate thermal vegetation stress, whereas high values reflect favourable thermal vegetation conditions.

Finally, the VHI is calculated from the VCI and the TCI (Bhuiyan *et al.* 2006). The VHI_r is composed of the VCI_r and TCI_r with the temporal resolution of r as follows:

$$VHI_r = a \cdot VCI_r + (1 - a) \cdot TCI_r, \quad (4)$$

a is often assumed to be 0.5, since the exact composition of the VHI from moisture and temperature is not known (Kogan *et al.* 2016). In addition, we test various a-values and determine the a-value with the highest correlation between VHI and olive oil yield. Table S2 in the Appendix shows the respective a-values of the provinces used to calculate the VHI.

The benchmark indices are calculated by summing the daily precipitation and temperature values (Dalhaus and Finger 2016; Turvey 2001) in order to obtain the same temporal resolution r as for the vegetation health indices. The temperature sum (T) and precipitation sum (P) are calculated as follows:

$$T^{t,c} = \sum_{r=1}^{x} T_r^{t,c}, \quad (5)$$

$$P^{t,c} = \sum_{r=1}^{x} P_r^{t,c}, \quad (6)$$

where the corresponding year is represented by t, r indicates the temporal resolution of the index accumulation period, c is an expression for the respective province and x expresses the length of the index calculation period (Jewson *et al.* 2005).

For the satellite indices (VCI, TCI, VHI), we use a slightly different approach than for the meteorological indices. Since the satellite indices are given by normalisation in the value range between 0 and 100, we use averages instead of sums. Index $SI^{t,c}$ represents the average values of the satellite indices used (Jewson *et al.* 2005):

$$SI^{t,c} = \frac{1}{x}\sum_{r=1}^{x} SI_r^{t,c}, \tag{7}$$

where $SI_r^{t,c}$ denotes the respective satellite index for the temporal resolution r, t corresponds to the year, c characterises the province under consideration and x provides information on the length of the index calculation period.

4. Copula approach for the design of weather index insurance

In order to model a flexible dependence structure between crop yield and indices, we use the copula approach for the design of weather index insurance. For this purpose, we model the marginal distribution of the olive oil yield as well as of the respective indices and we estimate the copula parameters. With the resulting parameters of both the marginal distributions and the copulas, we design the weather index contracts before determining their hedging effectiveness.

4.1 Flexible dependence with copulas

The underlying idea beyond the concept of weather index insurance is the payment of indemnity as soon as the weather index falls below/exceeds a critical threshold. Numerous studies use linear regression for the design of a weather index insurance in order to determine the relationship between the crop yield and a weather index (Berg and Schmitz 2008; Breustedt *et al.* 2008; Conradt *et al.* 2015). However, regression analyses contain some limited assumptions. For example, assuming a linear dependence in the tails of a joint distribution function of crop yield and weather index is not appropriate to assess extreme weather influences on yield (McNeil *et al.* 2015). For this reason, especially in the financial and insurance sectors, the copula method is proposed for the representation of multivariate dependency structures. Copulas are used to model the marginal behaviour of the random variables separately and allow flexibility in the description and estimation of margins (Reboredo 2011). Also in the area of agricultural economics, several studies have already used the copula approach to design and rate weather index insurance (Bokusheva 2011; Martínez Salgueiro 2019; Nguyen-Huy *et al.* 2018; Vedenov 2008; Woodard et al. 2011).

The copula method is based on Sklar's theorem (Sklar 1959). Accordingly, a copula $C:[0,1]^d \rightarrow [0,1]$ exists if $F_1,\ldots,F_d$ are the marginal distributions from the joint distribution function F. This applies to all random variables d from the vector $x_1,\ldots,x_d$ from $\overline{R} = [-\infty,\infty]$ as shown below:

$$F(x_1,\ldots,x_d) = C(F_1(x_1),\ldots,F_d(x_d)). \quad (8)$$

The idea behind the copula method is that through the marginal distributions $F_1,\ldots,F_d$ and the copula C information about the dependency structure can be gained. This is done by combining the marginal distributions in a joint distribution function (Embrechts *et al.* 2002).

4.2 Estimating of marginal distributions and copula parameter

In this study, we calculate the copula dependence parameter between the olive oil yield and the respective indices for the most critical periods[2] of the olive trees' vegetation cycle. The calculation of the copula parameters is done in two steps. First, we calculate the parameters of the marginal distributions for the olive oil yield and the different indices in each province by fitting different parametric distributions. We consider the following distributions: Normal, Log-normal, Logistic, Gamma and Weibull. The best fitting distributions for the indices and the olive oil yield are determined by Kolmogorov–Smirnov and Anderson–Darling tests. In the second step, we estimate the parameters of the copula function using the Kendall's tau estimation method (Genest *et al.* 2011). We calculate the Clayton, Frank and survival Gumbel to model dependence for the VCI, TCI, VHI and precipitation, given that the correlation between the yield and these indices is positive. In the case of temperature, we consider the 270 degree rotated Clayton, the Frank and the 90 degree rotated Gumbel, since the correlation of this variable to the yield is negative. The Gaussian and Frank copula are characterised by an almost identical dependence structure over the joint distribution function, which is equally reinforced only in the extreme left and right tail, while the Clayton and survival Gumbel copula have a strong dependence structure in the left tail of the joint distribution function (Nelsen 2006). We apply the AIC (Akaike information criterion) to find the most suitable copula to represent the yield-index dependence structure. For a comparison, we also apply the Gaussian copula, which assumes linear dependency.

4.3 Design of weather index insurance

For the design of the weather index insurance contracts, 1,000 simulated pairs of olive oil yields and respective index values are generated. The simulation is

[2] As in the study by Bokusheva *et al.* (2016), the critical phases of olive vegetation with the greatest dependence between the respective index and the olive yields were measured by the Spearman correlation coefficient.

based on the distributions chosen to model the marginals and on the resulting parameter of the most suitable copula.

In our study, we use the concept of the Marginal Expected Shortfall (MES) to model weather index insurance contracts according to the approach suggested by Mainik and Schaanning (2012). The MES specifies the Expected Shortfall (ES) of the crop yield depending on a weather index, if the weather index falls below or exceeds a certain threshold value. In our calculations, we determine separate MES of the crop yield for each realisation of the index value below the threshold value to set the insurance contract parameters in the following. Consequently, in the case of a positive correlation between the index and the yield, we focus on the expected shortfall value of the conditional yield $\mu^*_{t,c}$ when the weather index W falls below a certain level, which is expressed in the following form:

$$\mu^*_{t,c} = MES_{t,c}\, Y_c | W_{t,c} = E(Y_c | W_{t,c} \leq q_p(W_c)), \tag{9}$$

where E denotes the expected value, Y is the olive yield, t stands for the year, c reflects the province, W is the index and can take the form of any of the satellite- or meteorological-based indices considered and q_p is the p-quantile, with $0 \leq p \leq 1$. Since we assume that the yield-index dependence structure is higher when negative extreme events occur and the weather index insurance only pays indemnities if an index falls below a certain value, we select p to be 0.3 (Bokusheva *et al.* 2016) when the correlation between yield and index is positive. Accordingly, when the correlation between the index and the yield is negative, we derive the expected shortfall value of the conditional yield $\mu^*_{t,c}$ if the index W exceeds a given threshold, which is expressed in the following form:

$$\mu^*_{t,c} = MES_{t,c}\, Y_c | W_{t,c} = E\Big(Y_c | W_{t,c} \geq q_{1-p}(W_c) \Big). \tag{10}$$

The expression $\mu^*_{t,c}$ is determined by modeling the distribution of the yield conditional on the realisations of the considered indices. Following Jiang (2012) and Eckernkemper (2018), in the case of a positive index-yield correlation $\mu^*_{t,c}$ is derived from the copula approach as follows:

$$\mu^*_{t,c} = \frac{1}{p} \int_0^1 q_u(Y_c) \frac{\partial C(u,p;\theta)}{\partial u} du, \tag{11}$$

where $q_u(Y_c)$ is the quantile function, u stands for the marginal distribution of the yield Y, p is the probability that corresponds to the p-quntile of the index W with $W \leq q_p(W)$ and θ denotes the copula parameter.

When the correlation between the index and the yield is negative, $\mu^*_{t,c}$ is redefined as:

$$\mu^*_{t,c} = \frac{1}{p}\int_0^1 q_u(Y_c)\left[1 - \frac{\partial C(u, 1-p;\theta)}{\partial u}\right]du. \tag{12}$$

Following Bokusheva (2018), we calculate the indemnity payments and the fair insurance premium[3] with the previously computed $\mu^*_{t,c}$ values. Concretely, when the correlation between the index (VCI, TCI, VHI and precipitation) and yield is positive the indemnity $I_{t,c}$ is determined as follows:

$$I_{t,c} = \begin{pmatrix} K - \mu^*_{t,c} & if\, W_{t,c} \le q_p(W_c) \\ 0 & otherwise \end{pmatrix}, \tag{13}$$

where the strike yield K is the historical average yield.
As the correlation between yield and temperature is negative, the indemnity for the temperature index is calculated as follows:

$$I_{t,c} = \begin{pmatrix} K - \mu^*_{t,c} & if\, W_{t,c} \ge q_{1-p}(W_c) \\ 0 & otherwise \end{pmatrix}. \tag{14}$$

The fair insurance premium P_c is directly calculated as the expected indemnity value $I_{t,c}$ from the number of observations N as follows:

$$P_c = \frac{1}{N}\sum_{t=1}^{N} I_{t,c}. \tag{15}$$

4.4 Hedging effectiveness

To assess the risk reducing potential of the insurance contracts, revenues are compared with and without weather index insurance. For reasons of simplification, indemnities and fair premiums are measured in units of quantity (kg/ha) rather than monetary units. In order to convert into monetary units, the units of quantity are simply multiplied by the price per unit of quantity (Skees *et al.* 1997). Consequently, we compare the uninsured and the resulting insured yield according to the following formula (Bokusheva 2018):

[3] The fair insurance premium does not include any administrative costs.

$$y_{t,c}^{insured} = y_{t,c} + I_{t,c} - P_c, \tag{16}$$

where $y_{t,c}$ is the uninsured yield, $I_{t,c}$ indicates the indemnity payment and P_c stands for the fair premium.

According to Vedenov and Barnett (2004), we determine the hedging effectiveness of insurance contracts by comparing the semi-variance (SV) of uninsured yields with the SV of insured yields. The downside risk measure SV_c is computed as follows:

$$SV_c = \frac{1}{N}\sum_{t=1}^{N}\left[min\left(y_{t,c} - \overline{y}_c, 0\right)\right]^2, \tag{17}$$

where $y_{t,c}$ is the insured or uninsured conditional yield at a given moment t for the province c and $\overline{y}_c$ is the uninsured average yield of the respective province. N, which denotes the number of observations of the sample, corresponds to the 1,000 simulated data points.

5. Study area and data

The study area of Andalusia generates 80 per cent of the Spanish olive production and 30 per cent of the world's olive production. Olive trees, especially those used for oil production, are the most important crop, since they occupy over 1.5 million hectares, about half of Andalusia's total agricultural area (UNESCO 2019). The study area comprises 5 of the 8 provinces of Andalusia, which is located in southern Spain. We select the provinces of Cordoba, Granada, Jaen, Malaga and Sevilla for our study as the area cultivated with olive trees is larger than 100,000 hectares in each of the 5 provinces. Figure 1 reveals the locations of the non-irrigated olive fields for each province.

The study region is characterised by heterogeneous areas with different production and structural attributes due to prevailing differences in terms of topography, soil and climate (see Figure S2 in the Appendix). The area around the Guadalquivir Valley in southern and central Sevilla and central Cordoba is a dry farming region with the main cultivation of wheat and soy on large farms, but olive growing is also gaining in importance. The region of southern Cordoba and central Jaen is characterised by its specialisation in olive growing, with the main area located in the province of Jaen. The olive cultivation ranges from high-yield lands with irrigation and intensive use of inputs to low-yield marginal lands with water shortages, poor soil quality and steep slopes. The mountain range of the Betic Cordilleras, which extends mainly over Granada and southern Jaen, has a heterogeneous structure with strong temperature fluctuations due to varying elevations and areas with low precipitation. The soils are affected by erosion and are rather unfavourable

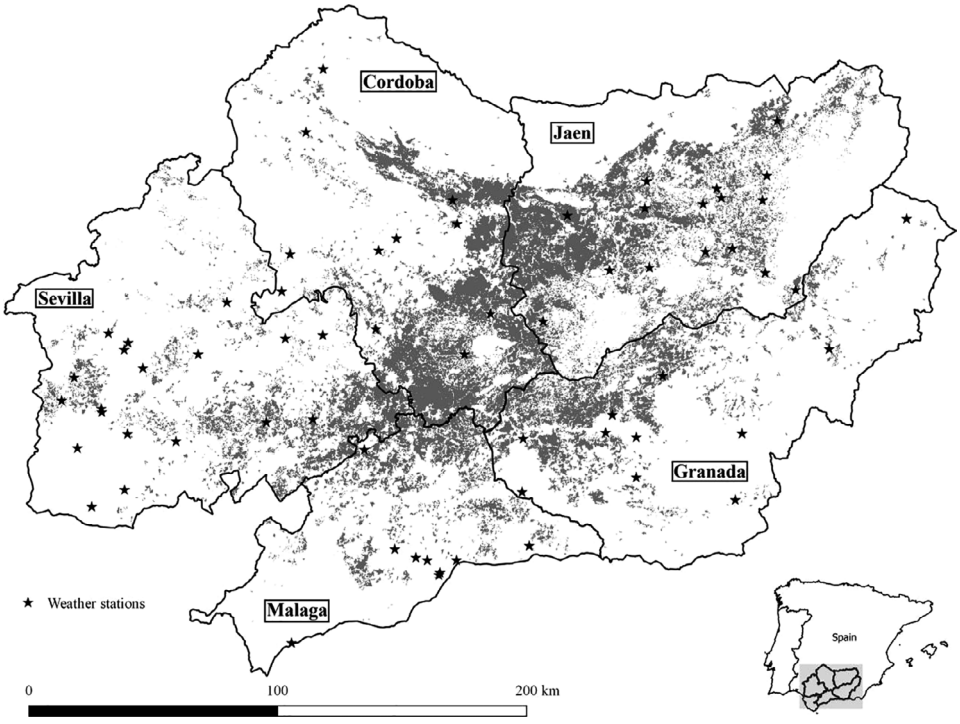

Figure 1 Fields with non-irrigated olive trees in 5 provinces of Andalusia. Source: Own presentation according to Land Monitoring Service (2012).

for agriculture. In the climatically milder areas between the mountains there are mainly low-yield cereal growing areas and dry farming areas with olive trees (Massot 2016).

In general, the Mediterranean climate in Andalusia, to which the olive trees are well adapted, is influenced by the Azores High and is therefore characterised by hot temperatures during dry summers. The average maximum temperature in July is 36.2 degrees Celsius, while it drops to only 14.8 degrees Celsius during the wintertime. Precipitation in Andalusia occurs mainly between November and April. On the coast, it is particularly rainy in November and December. The summer months are generally dry. Furthermore, the average amount of precipitation decreases continuously towards the east coast due to the decreasing influence of the Atlantic Ocean (Climate-Data 2019). The annual olive growing cycle can be characterised by the four phenological phases: inflorescence development, flowering, fruit growth and oil accumulation (see Figure S1 in the Appendix). While inflorescence development and flowering take place mainly in March, April and May, fruit growth is most strongly influenced in the period from May to October. The main oil accumulation phase ranges between the months of August and November. Between November and March, the olives are harvested, depending on the location, the weather and the variety of olives (Alarcon

2014). Although the phenological growth stages within each culture are the same, the time of occurrence of the respective stages depends on the olive variety, the location and the year (Sanz-Cortes *et al*. 2002).

The meteorological temperature and precipitation data are provided by the Spanish Meteorological Agency (AEMET) and by the Institute for Research and Education for Agriculture and Fisheries (IFAPA) of Junta de Andalucía. The weather stations are distributed over the respective provinces (see Figure 1). While in Malaga the available meteorological data are measured at 9 weather stations for the years from 2000 to 2015, in Sevilla we take the data from 19 weather stations. The aggregated weather station data used for each province are calculated from the average of the individual weather station values. The satellite data are recorded by a MODerate-resolution Imaging Spectroradiometer (MODIS) installed on the Terra satellite. The MODIS instruments measure 36 spectral bands between 0.405 and 14.385 μm in three different spatial resolutions (250 m, 500 m and 1,000 m) (MODIS 2019). For the calculation of the VCI, the MODIS product MOD13Q1 is selected, which provides EVI images with a spatial resolution of 250 × 250 m in a temporal sequence of 16 days. All images are adjusted for cloud contamination. Thus, only pixel values with a high pixel accuracy are included in the calculations. The LST for the TCI are obtained from the observation product MOD11A2. Day temperatures, recorded around 12 pm, are chosen for our analyses, because yield losses are more often a result of high daytime temperatures than nighttime temperatures (Gibson and Mullen 1996). The temporal resolution of the LST product amounts to 8 days while the spatial resolution is 1,000 × 1,000 m. The LST images are also adjusted for cloud contamination. Furthermore, the pixels with an LST error of more than 4 Kelvin are removed. To obtain the 16-day resolution of the EVI values, we aggregate the LST values using the average of two 8 day LST images. Thus, in our investigations the satellite indices (formula 2, 3 and 4) and the precipitation and temperature indices (formula 5 and 6) have a temporal resolution r of 16 days.

Figure 2 shows the 16-day values of the VCI, TCI and VHI for the province of Cordoba. The satellite indices reach their annual peaks on average over the years 2000 to 2015 on day 1 for the TCI and VHI or on day 81 in the case of the VCI, whereas the annual lows are reached in midsummer on day 193 for the TCI, on day 209 for the VHI or on day 225 for the VCI. It can be seen that the TCI varies much more strongly than the VCI over the course of the year. In addition, TCI values start to rise earlier and faster than VCI values.

To identify the fields cultivated with olive trees, we apply the 2012 CORINE Land Cover layer, which identified the olive trees by using dual date images from the satellites Resourcesat-1 and RapidEye, achieving a thematic accuracy of over 85 per cent (Land Monitoring Service 2012). Since we are using weather index insurance to investigate alternative options for risk management, we only include non-irrigated olive tree fields in the

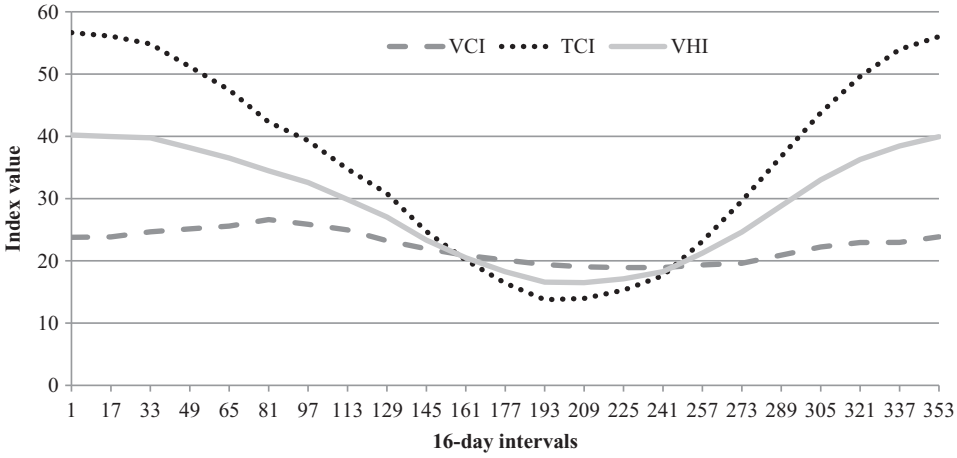

Figure 2 Sixteen-day values of the VCI, TCI and VHI on average over the years 2000 to 2015 for the province of Cordoba.

calculations, so that we distinguish between irrigated and non-irrigated fields. For this purpose we use the VCI for a high accuracy in the determination of the non-irrigated fields, because the pixel resolution of the TCI is lower. For the classification, we use single-date images (Ozdogan *et al.* 2010). Thus, the observation date, on which the difference in the VCI values between irrigated and non-irrigated olive areas is greatest, must be determined (Chance *et al.* 2017). Depending on the year, the VCI values show their annual minimum values in the months of July and August (see Figure 2), as this is the period with the lowest precipitation and highest temperatures (Climate-Data 2019). Therefore, we assume that irrigation has the strongest effect on the VCI values in this period. We chose the satellite image of day 225 from the year 2012 for the distinction, because at that time the lowest precipitation of the entire investigation period was recorded. We set a separate threshold for each province, which is contained in the data set and indicates the percentage of non-irrigated olive groves in each province. Then we determine which VCI value corresponds to the threshold quantile of the entire value range of the VCI, so that all pixels with lower VCI values than the threshold are classified as non-irrigated fields[4]. On average, 30 percent of the fields in Andalusia are irrigated, so that depending on the province, about 70 percent of the VCI pixel values are classified as non-irrigated fields (Massot 2016).

[4] To verify our results, we have repeated the calculations using the TCI. We find that non-irrigated areas have a higher surface temperature than the irrigated ones due to the lack of evaporation cooling (Wu and De Pauw 2011). We also calculated the correlations between the precipitation and temperature values and the VCI values for the identified non-irrigated and irrigated olive areas. The results show that the correlations between precipitation or temperature values and the VCI values of the non-irrigated olive areas are greater than the correlations with the VCI values of the irrigated olive areas (see Table S3 in the appendix).

The yield data are provided by the Spanish Ministry of Agriculture, Fisheries and Food (Ministerio de Agricultura, Pesca y Alimentación), whereby the data set contains the average olive oil yields of all irrigated olive trees as well as the average olive oil yields of all non-irrigated olive trees in Cordoba, Granada, Jaen, Malaga and Sevilla. Figure 3 shows the olive yields of the five provinces from year 2000 to year 2015. It can be observed that the olive oil yields vary relatively strongly in the observation period.

In accordance with the yield data, the satellite and meteorological indices are also calculated for the years 2000 to 2015. In Table S1 in the Appendix, summary statistics of olive oil yields, satellite indices as well as precipitation and temperature distributions are included.

6. Results

6.1 Decisive vegetation stages

The first step of our empirical investigation requires assessing the relationship between the indices and the olive oil yields and determining the vegetation periods with the strongest relationship. Table 1 reveals the dependency parameters of the considered copulas.

For the different provinces and indices, we find different periods that have the strongest relationship with the olive oil yields. It can be observed that the differences between the provinces are greater than between the indices, so that similar periods are found for the indices in the provinces. For Cordoba and Sevilla, the strongest relationship for the VCI with the olive oil yield exists in August (day 225). While we also identified August (day 241) for the TCI in

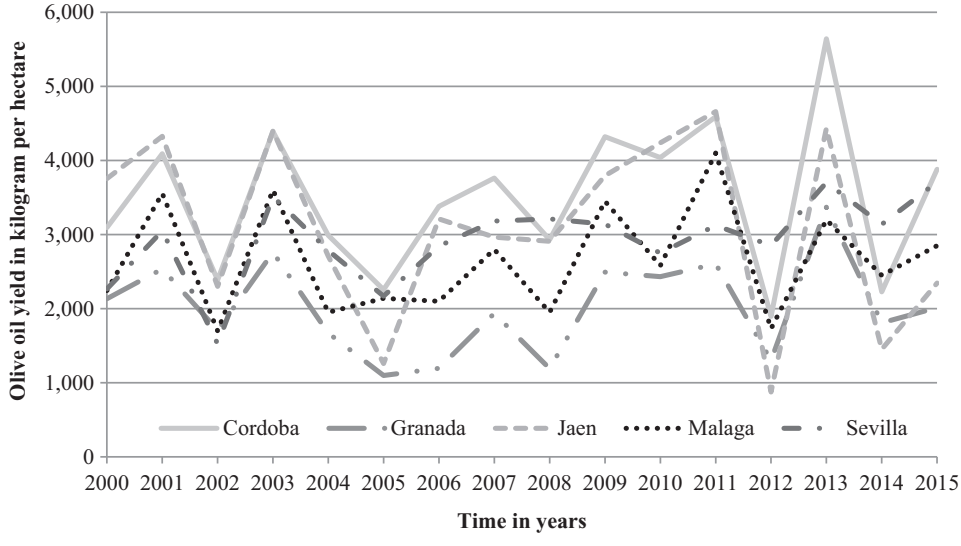

Figure 3 Olive oil yield data from 5 provinces in Andalusia from 2000 to 2015.

Table 1 Copula dependency parameters between olive oil yield and the respective index of the individual provinces

Province	Days of the year	Gaussian	Clayton[†]	Frank	Survival Gumbel[‡]
VCI					
Cordoba	225	0.67	1.75	5.16	1.88
Granada	81	0.59	1.33	4.16	1.67
Jaen	65–81	0.67	1.75	5.16	1.88
Malaga	65–81	0.66	1.71	5.06	1.85
Sevilla	225	0.69	1.87	5.44	1.94
TCI					
Cordoba	241	0.43	0.79	2.73	1.40
Granada	81	0.63	1.53	4.64	1.76
Jaen	81	0.69	1.87	5.44	1.94
Malaga	65–81	0.35	0.58	2.12	1.29
Sevilla	241–273	0.52	1.08	3.51	1.54
VHI					
Cordoba	113–129	0.63	1.53	4.64	1.76
Granada	81	0.76	2.44	6.73	2.22
Jaen	81	0.71	2.00	5.74	2.00
Malaga	65–81	0.64	1.59	4.79	1.80
Sevilla	241	0.67	1.75	5.16	1.88
Precipitation					
Cordoba	161–241	0.59	1.33	4.16	1.67
Granada	81–97	0.50	1.00	3.31	1.50
Jaen	65–225	0.54	1.16	3.72	1.58
Malaga	145–161	0.27	0.43	1.62	1.21
Sevilla	193–209	0.59	1.35	4.21	1.68
Temperature					
Cordoba	209	−0.28	−0.45	−1.70	−1.22
Granada	129	−0.41	−0.73	−2.55	−1.36
Jaen	129–145	−0.36	−0.61	−2.20	−1.30
Malaga	81	−0.27	−0.43	−1.62	−1.21
Sevilla	161–177	−0.45	−0.86	−2.92	−1.43

Note: [†]Rotated 270 degrees Clayton for temperature.
[‡]Rotated 90 degrees Gumbel for temperature.

Cordoba, the months of August and September (day 241-273) are the relevant months for the TCI in Sevilla. In the case of the VHI, the highest relationship with the olive oil yield exists in Sevilla in August (day 241). In the months of August and September (see Figure S1 in the Appendix), the fruits are still growing and olive oil is assimilated. In Cordoba the strongest relationship with the olive oil yield seems to be for the VHI during the period 113-129. In this vegetation phase the olive trees are in bloom. In contrast, in Granada, Jaen and Malaga, the greatest relationship between satellite indices and olive yield already exists in March (day 65 to 81 in the year). In March, the inflorescence development of the olive trees takes place (see Figure S1 in the Appendix). For precipitation and temperature, the periods with the highest dependence differ more between provinces. Nevertheless, the meteorological indices cover similar periods from day 81 to day 241 for the respective indices. In Cordoba and Sevilla, precipitation and temperature also seem to have the

strongest relationship with olive oil yield several weeks later than in Granada, Jaen and Malaga. For example, the temperature in Granada and Jaen has the greatest influence on the olive yield in May, which corresponds to olive flowering time (see Figure S1 in the Appendix), while in Cordoba (day 209) and Sevilla (day 161–177) this was the case for the phase of fruit development.

Besides the vegetation periods, Table 1 also shows that there is a strong relationship in the joint distributions of the considered indices and the olive oil yields. The Gaussian parameters[5] for the VCI reach values between 0.59 and 0.69, for the TCI between 0.35 and 0.69 and for the VHI between 0.63 and 0.76, depending on the province. In contrast, the parameters for precipitation range from 0.27 to 0.59 and for temperature from −0.27 to −0.45. Thus, on average, the relationship between the satellite indices and olive oil yields is greater than between the meteorological indices and olive oil yields. While the dependence strength varies least between provinces in the case of the VCI, the TCI has the greatest differences between provinces. Table 1 shows a similar dependence structure between the indices and the olive oil yield across all copula kinds despite different value ranges[6]. Stronger dependencies are represented by higher values of copula dependency parameters.

6.2 Hedging effectiveness

Using the AIC criterion, we select the best fitting copula for each distribution function of the respective index parameter and olive oil yield. The results show that survival Gumbel copula is best suited for all indices to determine the dependency structure between the respective index and olive oil yield. Furthermore, we determine the hedging effectiveness for the Gaussian copula to show the differences between a linear dependency structure and a strong tail dependency.

For the purposes of illustration, Figure 4 shows the copula density of the Gaussian and survival Gumbel copula for the 1,000 simulated values and a calculated Kendall´s tau of 0.47 between the VCI und the olive oil yield in Cordoba. The represented copula density is determined by the marginal distributions of the *VCI* and the *olive oil yield*. Compared to the Gaussian copula, the survival Gumbel copula has a stronger dependence in the left tail of the joint distribution. As weather index insurance is more likely to cover extreme weather events, the possibility to map an increased dependence in the left tail of the joint distribution is of particular interest.

Table 2 shows the hedging effectiveness of the weather index insurance contracts based on the different indices for each province. The results show

[5] The Gaussian copula is very similar to the Spearman correlation, since the Gaussian is a copula with linear dependencies.

[6] The different copula have the following value ranges: Gaussian copula [−1, 1], Clayton copula [− 1, ∞) \{ 0}, Frank copula [− ∞, ∞) \{ 0}, Gumbel copula [1, ∞).

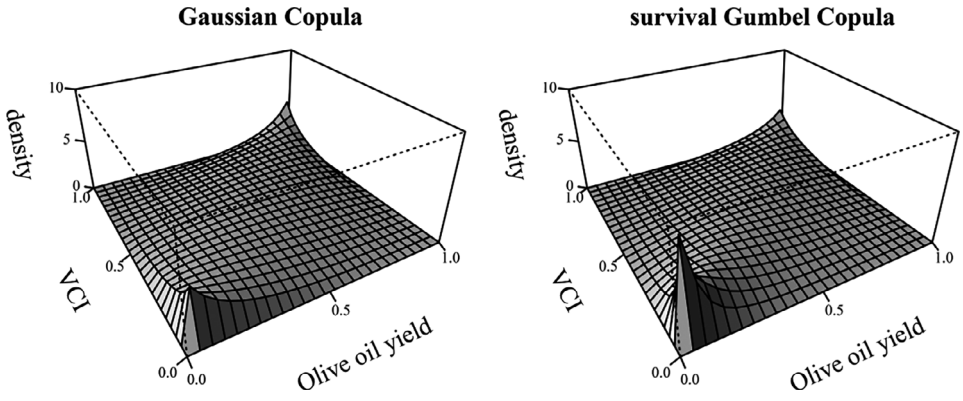

Figure 4 Comparison of the Gaussian and survival Gumbel copula density resulting from 1,000 simulated values and Kendall's tau of 0.47 between the VCI and the olive oil yield in Cordoba.

that the hedging effectiveness of the insurance contracts is positive. Furthermore, the results confirm that the survival Gumbel copula has, in most cases, a higher hedging effectiveness for the indices than the Gaussian copula due to its stronger dependence in the left tail of the joint distribution function.

The hedging effectiveness varies considerably among indices and provinces. Using the survival Gumbel copula, VCI- and VHI-based insurance contracts have the highest average hedging effectiveness with 38 per cent respectively. The average hedging effectiveness for the survival Gumbel copula of the TCI-based insurance contracts amounts to 29 per cent. VCI-, TCI- and VHI-based insurance contracts show a considerably higher hedging effectiveness than temperature-based insurance contracts (16 per cent). Compared to precipitation-based insurance contracts (29 per cent), VCI- and VHI-based insurance contracts have a higher hedging effectiveness. Since a higher

Table 2 Relative hedging effectiveness of the meteorological- and satellite-based weather index insurance contracts

Parameter	Copula	Cordoba	Granada	Jaen	Malaga	Sevilla	Average
VCI	Gaussian	0.29	0.20	0.28	0.30	0.35	0.29
	Gumbel†	0.42	0.31	0.42	0.34	0.43	0.38
TCI	Gaussian	0.16	0.29	0.28	0.09	0.16	0.20
	Gumbel†	0.25	0.36	0.47	0.08	0.29	0.29
VHI	Gaussian	0.30	0.39	0.35	0.28	0.29	0.32
	Gumbel†	0.25	0.52	0.44	0.26	0.43	0.38
Precipitation	Gaussian	0.20	0.15	0.23	0.05	0.21	0.17
	Gumbel†	0.35	0.28	0.31	0.09	0.41	0.29
Temperature	Gaussian	0.06	0.15	0.11	0.09	0.09	0.10
	Gumbel‡	0.12	0.16	0.14	0.15	0.22	0.16

Note: †Survival Gumbel.
‡Rotated 90 degrees Gumbel.

hedging effectiveness corresponds to a lower basis risk, our results show that satellite-based weather index insurance contracts have a lower basis risk than weather station-based weather index insurance contracts for the insurance of olive yields.

7. Discussion

Although olive trees are well adapted to low precipitation, olive yields in Andalusia are highly dependent on this meteorological variable. Our study shows a strong relationship between olive oil yields and the satellite indices. The results suggest that satellite-based weather index insurance contracts in particular appear to be suitable to hedge the risk of olive oil yields. Consequently, the hedging effectiveness of meteorological-based insurance contracts can be exceeded by using satellite indices.

However, there are differences between the individual provinces in stages of vegetation which are most closely linked to the olive oil yield and in the hedging effectiveness of the individual index-based insurance contracts. The differences may be due to the geographical situation of the provinces under consideration. Andalusia has varied climatic conditions due to its wide geographical area and the surface characteristics with large differences in altitude. Thus, moist Atlantic air penetrates through the Guadalquivir valley, which runs through Sevilla and Cordoba. Due to the low altitude (see Figure S2 in the Appendix), a subcontinental Mediterranean climate with hot summers prevails here (Massot 2016). In contrast, the provinces of Granada, Jaen and Malaga are characterised by a mountainous landscape with high altitudes. The precipitation density in Andalusia decreases from west to east (see Table S1 in the Appendix). Furthermore, the climate becomes more continental with rising mean altitude and increasing distance to the coast, whereby the temperature differences become larger (Massot 2016).

The geographical location and varying topography lead to different weather conditions in each of the provinces. The correlation between EVI and LST values can be used to validate the suitability of vegetation health indices. If there is a negative correlation, moisture would act as a limiting factor for plant growth. In contrast, if there is a positive correlation between EVI and LST values, temperature as a form of energy would become the limiting factor which is typical in higher elevations (Karnieli *et al.* 2010). The following correlations between EVI and LST values exist in our study area: −0.66 (Cordoba), −0.37 (Granada), −0.62 (Jaen), −0.70 (Malaga) and −0.78 (Sevilla). The correlations are negative in all provinces, which indicate that moisture is the most relevant limiting factor for the vegetation. The provinces of Granada and Jaen have higher hedging effectiveness than Cordoba, Malaga and Sevilla in the case of TCI-based insurance contracts. However, the correlations between EVI and LST values show the lowest negative correlations in Granada (−0.37) and Jaen (−0.62), indicating that water is a less limiting factor than in the other provinces. On the contrary, the

temperature is determined by the altitude (see Figure S2 in the Appendix) and the higher temperature fluctuations here are due to the increase in the average altitude in these provinces (Massot 2016). For VCI-based insurance contracts, the province of Granada has the lowest hedging effectiveness with 31 per cent. The landscape in Granada is very mountainous and has high altitudes (see Figure S2 in the Appendix), which reduces the vegetation. Furthermore, the VCI is strongly correlated with the amount of precipitation (Rojas *et al.* 2011). In Granada, precipitation does not limit yields as much as in the other provinces, as the correlation between EVI and LST values is not quite as strong at −0.37. Consequently, it can be stated that in higher altitudes TCI-based insurance contracts are superior to VCI-based insurance contracts. The VHI values were determined using the *a*-values best suited to each province. In provinces with a higher altitude such as Granada and Jaen, the percentage share of the TCI in the VHI is greater (see Table S2 in the Appendix). VHI-based insurance contracts have a high hedging effectiveness in provinces with higher altitudes, which are also affected by greater temperature fluctuations due to their eastern location in Andalusia (Massot 2016). In Granada and Jaen, VHI-based insurance contracts have a hedging effectiveness of 52 per cent and 44 per cent, respectively. Thus, VHI-based insurance contracts also have considerably higher hedging effectiveness than precipitation- and temperature-based insurance contracts in such provinces.

Nevertheless, the hedging effectiveness of satellite-based insurance contracts also depends on the proportion of cultivated land per pixel of the satellite images. Therefore, it must be mentioned that the exact location of the olive groves is unknown. The identification of the olive fields has an accuracy of approximately 85 per cent (Land Monitoring Service 2012). However, utilising satellite data with a higher spatial resolution (e.g. Copernicus satellites such as Sentinel 2) could improve the accuracy of olive field identification. In addition, the use of satellite data with a higher spatial resolution would lead to further reduction of basis risk of spatial resolution, as defined by Möllmann *et al.* (2019), which could further increase the hedging effectiveness of satellite-based insurance contracts.

In the case of precipitation- and temperature-based insurance contracts, no major differences in the hedging effectiveness can be observed between the provinces. Only in Malaga does the hedging effectiveness of precipitation-based insurance contracts (with 9 per cent) differ strongly from the other provinces. However, the coverage with weather stations used for the calculation of the meteorological indices is very low in Malaga, so there are sometimes large distances between the olive grove fields and the weather stations (see Figure 1). Thus, the advantages of satellite indices over weather station data are particularly pronounced in regions of the earth with a sparse network of weather stations.

This study makes an initial proposal to hedge the high yield risk of perennial plantation crops such as olive trees through satellite-based weather index insurance. The study shows that satellite-based index insurance

outperform meteorological-based index insurance and thus satellite-based index insurance can be an effective alternative for risk management. In Andalusia, about 70 per cent of the olive groves are not irrigated, so the majority of the olive trees are exposed to drought. Against this background, this study shows that satellite-based weather index insurance contracts could offer the possibility for olive farmers to hedge the yield variability of non-irrigated olive groves by means of indemnity payments. The focus and results of our study are interesting not only to olive farmers but also for policymakers. In the future, alternatives to the irrigation of olive groves in Andalusia will be necessary, as the availability of water becomes more and more problematic and expensive due to the intensified cultivation of irrigated olive groves. Therefore, the political agenda for the budgetary allocations in Spain focuses on strengthening efficient and sustainable production, maintaining natural resources and limiting their exploitation (Martínez and Almonacid 2017). However, Quiroga and Iglesias (2009) point out that the promotion of insurance in the context of the Common Agricultural Policy (CAP) requires better tools for quantification of climate-crop interactions. In our study, insurance contracts calculated with the survival Gumbel copula show higher hedging effectiveness compared to the Gaussian copula. As we design the insurance contracts for the lower range of the underlying vegetation health indices, it can be concluded that the relationship between the indices and the olive oil yield is characterised by tail dependence. Consequently, there is a particularly strong relationship between negative weather conditions and the olive oil yield, since the survival Gumbel copula, in contrast to the Gaussian copula, has a stronger dependence structure in the left tail of the joint distribution function. Thus, this study is also relevant for potential providers of weather index insurance.

Consequently, satellite-based index insurance designed against extreme weather events could encourage farmers to abandon unsustainable practices, as index insurance can also cover yield losses in extreme weather situations where technological options can only counteract weather-related yield losses to a limited extent (Bokusheva 2018).

8. Conclusion

Weather index insurance could help to hedge against extreme heat and drought. However, classic weather index insurance have so far hardly been applied in the insurance sector, as the common meteorological indices rarely reflect yield due to a high basis risk (Smith and Watts 2012). Since satellite indices are not dependent on proximity to a weather station and are available free of charge for any region worldwide, they could help to reduce the basis risk.

In this paper, we design weather index insurance contracts based on satellite indices for all non-irrigated olive fields located in 5 provinces of Andalusia and investigate whether it is possible to hedge yield risks from olive oil cultivation with these index insurance contracts. In addition to the satellite indices VCI, TCI

and VHI, we also consider precipitation and temperature indices as benchmarks. We use relatively high-resolution MODIS satellite data and average olive oil yields at provincial level. Furthermore, we apply a copula approach to determine tail dependence between the olive oil yield and the indices.

Our results show that the relationship between the olive oil yields and the indices considered is most pronounced for the phases of inflorescence development, flowering, fruit growth and oil accumulation. Using the survival Gumbel copula, the VCI- and VHI-based insurance contracts have an average hedging effectiveness of 38 per cent and greatly outperform temperature- and precipitation-based insurance contracts (16 per cent or 29 per cent). Moreover, with an average hedging effectiveness of 29 per cent TCI-based insurance contracts greatly outperform temperature-based insurance contracts. However, there are differences between the respective provinces. While VCI-based insurance contracts tend to have a strong hedging effectiveness for provinces in lower altitudes, TCI- and VHI-based insurance contracts appear to be more suitable for provinces in mountainous altitudes. Since higher hedging effectiveness is attributable to a lower basis risk, we can conclude that satellite-based insurance contracts have a lower basis risk than the meteorological-based insurance contracts.

These findings suggest that satellite-based weather index insurance can be a risk management alternative to hedge the risk to olive oil yields. However, in addition to regional characteristics, the effect of satellite-based weather index insurance contracts depends strongly on the quality of satellite and yield data. In addition to the use of satellite imagery with a higher spatial resolution, future studies could determine the critical index calculation periods of olive cultivation based on satellite data to take into account the annual variations in the beginning and end of vegetation periods. For future research, less aggregated data should serve as a basis for olive oil yields. The hedging effectiveness of the satellite indices will presumably still improve, since there is a natural compensation of risk within the provinces. Since the results do not allow any conclusions to be drawn about the willingness to pay (WTP) of farmers for such insurances, subsequent studies using farm-level yields should also look into other economic issues such as the WTP of farmers for such insurances at cost-covering insurance premiums for potential providers of weather index insurance.

Data availability statement

The authors declare that the data are not publicly available.

References

Alarcon, J.J. (2014). *Guidelines on Best Irrigation Management Practices for Olive Production in the Mediterranean Area. Sustainable Use of Irrigation Water in the Mediterranean Region, Theme 2: Biotechnologies, Agriculture, Food.* Seventh Framework Porgramme, Brussels.

Ashenfelter, O. and Storchmann, K. (2010). Measuring the economic effect of global warming on viticulture using auction, retail, and wholesale prices, *Review of Industrial Organization* 37, 51–64.

Barnett, B. and Mahul, O. (2007). Weather index insurance for agriculture and rural areas in lowerincome countries, *American Journal of Agricultural Economics* 89, 1241–1247.

Berg, E. and Schmitz, B. (2008). Weather-based instruments in the context of whole-farm risk management, *Agricultural Finance Review* 68, 119–133.

Bhuiyan, C., Singh, R.P. and Kogan, F.N. (2006). Monitoring drought dynamics in the Aravalli region (India) using different indices based on ground and remote sensing data, *International Journal of Applied Earth Observation and Geoinformation* 8, 289–302.

Boehm, R., Cash, S., Anderson, B., Ahmed, S., Griffin, T., Robbat, A., Stepp, J., Han, W., Hazel, M. and Orians, C. (2016). Association between empirically estimated monsoon dynamics and other weather factors and historical tea yields in China: Results from a yield response model, *Climate* 4, 20.

Bokusheva, R. (2011). Measuring dependence in joint distributions of yield and weather variables, *Agricultural Finance Review* 71, 120–141.

Bokusheva, R. (2018). Using copulas for rating weather index insurance contracts, *Journal of Applied Statistics* 45, 2328–2356.

Bokusheva, R. and Breustedt, G. (2012). The effectiveness of weather-based index insurance and areayield crop insurance: How reliable are ex post predictions for yield risk reduction? *Quarterly Journal of International Agriculture* 51, 135–156.

Bokusheva, R., Kogan, F., Vitkovskaya, I., Conradt, S. and Batyrbayeva, M. (2016). Satellite-based vegetation health indices as a criteria for insuring against drought-related yield losses, *Agricultural and Forest Meteorology* 220, 200–206.

Breustedt, G., Bokusheva, R. and Heidelbach, O. (2008). Evaluating the potential of index insurance schemes to reduce crop yield risk in an arid region, *Journal of Agricultural Economics* 59, 312–328.

Brilli, L., Chiesi, M., Maselli, F., Moriondo, M., Gioli, B., Toscano, P., Zaldei, A. and Bindi, M. (2013). Simulation of olive grove gross primary production by the combination of ground and multi-sensor satellite data, *International Journal of Applied Earth Observation and Geoinformation* 23, 29–36.

Chance, E., Cobourn, K., Thomas, V., Dawson, B. and Flores, A. (2017). Identifying irrigated areas in the snake river plain, Idaho: evaluating performance across composting algorithms, spectral indices, and sensors, *Remote Sensing* 9, 546.

Chantarat, S., Mude, A.G., Barrett, C.B. and Carter, M.R. (2013). Designing index-based livestock insurance for managing asset risk in Northern Kenya, *Journal of Risk and Insurance* 80, 205–237.

Climate-Data (2019). Climate: Andalusia. Available from URL: https://en.climate-data.org/europe/spain/andalusia-252/ [accessed 20 January 2019].

Collier, B., Skees, J. and Barnett, B. (2009). Weather index insurance and climate change: Opportunities and challenges in lower income countries, *The Geneva Papers on Risk and Insurance - Issues and Practice* 34, 401–424.

Conradt, S., Finger, R. and Bokusheva, R. (2015). Tailored to the extremes: Quantile regression for index-based insurance contract design, *Agricultural Economics* 46, 537–547.

Dalhaus, T. and Finger, R. (2016). Can gridded precipitation data and phenological observations reduce basis risk of weather index-based insurance?, *Weather, Climate, and Society* 8, 409–419.

Deschenes, O. and Kolstad, C. (2011). Economic impacts of climate change on California agriculture, *Climatic Change* 109, 365–386.

Didan, K., Munoz, A.B., Solano, R. and Huete, A. (2015). MODIS vegetation index user´s guide (MOD13 Series). Vegetation Index and Phenology Lab. *The University of Arizona*.

Eckernkemper, T. (2018). Modeling systemic risk: time-varying tail dependence when forecasting marginal expected shortfall, *Journal of Financial Econometrics* 16, 63–117.

Embrechts, P., McNeil, A. and Straumann, D. (2002). Correlation and dependence in risk management: Properties and pitfalls, in Dempster, M.A.H. (ed), *Risk Management: Value at Risk Beyond*, Cambridge, pp. 176–223.

Genest, C., Nešlehová, J. and Ben Ghorbal, N. (2011). Estimators based on kendall's tau in multivariate copula models, *Australian & New Zealand Journal of Statistics* 53, 157–177.

Gibson, L.R. and Mullen, R.E. (1996). Influence of day and night temperature on soybean seed yield, *Crop Science* 36, 98.

Gommes, R. and Göbel, W. (2013). Beyond simple, one-station rainfall indices, in Gommes, R. and Kayitakire, F. (eds), *The Challenges of Index-based Insurance for Food Security in Developing Countries*. European Union Publications, Luxembourg, pp. 205–221.

Goodwin, B.K. (2001). Problems with market insurance in agriculture, *American Journal of Agricultural Economics* 83, 643–649.

Gunathilaka, R.P.D., Smart, J.C.R. and Fleming, C.M. (2017). The impact of changing climate on perennial crops: the case of tea production in Sri Lanka, *Climatic Change* 140, 577–592.

Gunathilaka, R.P.D., Smart, J.C.R. and Fleming, C.M. (2018a). Adaptation to climate change in perennial cropping systems: Options, barriers and policy implications, *Environmental Science & Policy* 82, 108–116.

Gunathilaka, R.P.D., Smart, J.C.R., Fleming, C.M. and Hasan, S. (2018b). The impact of climate change on labour demand in the plantation sector: the case of tea production in Sri Lanka, *Australian Journal of Agricultural and Resource Economics* 62, 480–500.

Jewson, S., Brix, A. and Ziehmann, C. (2005). *Weather Derivative Valuation: The Meteorological, Statistical, Financial and Mathematical Foundations*. Cambridge University Press, Cambridge, UK.

Jiang, C. (2012). Does Tail Dependence Make A Difference In the Estimation of Systemic Risk? Δ CoV aR and MES. Working Paper, Economics Department, Boston College, MA.

Kapphan, I., Calanca, P. and Holzkaemper, A. (2012). Climate change, weather insurance design and hedging effectiveness, *Geneva Papers on Risk and Insurance: Issues and Practice*. 37, 286–317.

Karnieli, A., Agam, N., Pinker, R.T., Anderson, M., Imhoff, M.L., Gutman, G.G., Panov, N. and Goldberg, A. (2010). Use of NDVI and land surface temperature for drought assessment: merits and limitations, *Journal of Climate* 23, 618–633.

Kogan, F. (1995). Droughts of the late 1980s in the United states as derived from NOAA Polar-Orbiting Satellite Data, *Bulletin of the American Meteorological Society* 76, 655–668.

Kogan, F. (1998). A typical pattern of vegetation conditions in southern Africa during El Nino years detected from AVHRR data using three-channel numerical index, *International Journal of Remote Sensing* 19, 3688–3694.

Kogan, F., Gitelson, A., Zakarin, E., Spivak, L. and Lebed, L. (2003). AVHRR-based spectral vegetation index for quantitative assessment of vegetation state and productivity, *Photogrammetric Engineering & Remote Sensing* 69, 899–906.

Kogan, F., Guo, W., Strashnaia, A., Kleshenko, A., Chub, O. and Virchenko, O. (2016). Modelling and prediction of crop losses from NOAA polar-orbiting operational satellites, *Geomatics, Natural Hazards and Risk* 7, 886–900.

Kogan, F., Salazar, L. and Roytman, L. (2012). Forecasting crop production using satellite-based vegetation health indices in Kansas, USA, *International Journal of Remote Sensing* 33, 2798–2814.

Land Monitoring Service (2012). Copernicus-CORINE land cover. CLC 2012. Available from URL: https://land.copernicus.eu/pan-european/corine-land-cover [accessed 28 January 2019].

Lavee, S., Nashef, M., Wodner, M. and Harshemesh, H. (1990). The effect of complementary irrigation added to old olive trees (*Olea europaea* L.) cv. Souri on fruit characteristics, yield and oil production, *Advances in Horticultural Science* 4, 135–138.

Leblois, A., Quirion, P., Alhassane, A. and Traoré, S. (2014). Weather index drought insurance: an ex ante evaluation for millet growers in Niger, *Environmental and Resource Economics* 57, 527–551.

Mainik, G. and Schaanning, E. (2012). On dependence consistency of CoVaR and some other systemic risk measures. Available from URL: http://arxiv.org/pdf/1207.3464v3 [accessed 10 January 2020].

Makaudze, E.M. and Miranda, M.J. (2010). Catastrophic drought insurance based on the remotely sensed normalised difference vegetation index for smallholder farmers in Zimbabwe, *Agrekon* 49, 418–432.

Martínez, J.D.S. and Almonacid, A.G. (2017). Productivism and post-productivism in the olive groves of southern Spain, *Quaestiones Geographicae* 36, 57–69.

Martínez Salgueiro, A. (2019). Weather index-based insurance as a meteorological risk management alternative in viticulture, *Wine Economics and Policy* 8, 114–126.

Massot, A. (2016). Research for AGRI Committee-Agriculture in Andalusia. Agriculture und Rural Development. *Directorate-General for internal policies*.

McNeil, A.J., Frey, R. and Embrechts, P. (2015). *Quantitative risk management: Concepts, techniques and tools, Princeton series in finance*, Revised edn. Princeton University Press, Princeton, Oxford.

Miranda, M.J. and Farrin, K. (2012). Index Insurance for developing countries, *Applied Economic Perspectives and Policy* 34, 391–427.

MODIS (2019). Moderate resolution imaging spectroradiometer. Available from URL: https://modis.gsfc.nasa.gov/data/ [accessed 28 January 2019].

Möllmann, J., Buchholz, M. and Musshoff, O. (2019). Comparing the hedging effectiveness of weather derivatives based on remotely sensed vegetation health indices and meteorological indices, *Weather, Climate, and Society* 11, 33–48.

Nelsen, R.B. (2006). *Introduction to Copulas, Springer Series in Statistics*, 2nd edn. Springer, New York, NY.

Nguyen-Huy, T., Deo, R.C., Mushtaq, S., Kath, J. and Khan, S. (2018). Copula-based agricultural conditional value-at-risk modelling for geographical diversifications in wheat farming portfolio management, *Weather and Climate Extremes* 21, 76–89.

Oteros, J., García-Mozo, H., Hervás, C. and Galán, C. (2013). Biometeorological and autoregressive indices for predicting olive pollen intensity, *International Journal of Biometeorology* 57, 307–316.

Ozdemir, Y. (2016). Effects of climate change on olive cultivation and table olive and olive oil quality, Scientific Papers. Series B, Horticulture, Volume LX.

Ozdogan, M., Yang, Y., Allez, G. and Cervantes, C. (2010). Remote sensing of irrigated agriculture: opportunities and challenges, *Remote Sensing* 2, 2274–2304.

Quiring, S.M. and Ganesh, S. (2010). Evaluating the utility of the Vegetation Condition Index (VCI) for monitoring meteorological drought in Texas, *Agricultural and Forest Meteorology* 150, 330–339.

Quiroga, S. and Iglesias, A. (2009). A comparison of the climate risks of cereal, citrus, grapevine and olive production in Spain, *Agricultural Systems* 101, 91–100.

Reboredo, J.C. (2011). How do crude oil prices co-move?, *Energy Economics* 33, 948–955.

Rojas, O., Vrieling, A. and Rembold, F. (2011). Assessing drought probability for agricultural areas in Africa with coarse resolution remote sensing imagery, *Remote Sensing of Environment* 115, 343–352.

Salazar, C., Jaime, M., Pinto, C. and Acuña, A. (2019). Interaction between crop insurance and technology adoption decisions: The case of wheat farmers in Chile, *Australian Journal of Agricultural and Resource Economics* 63, 593–619.

Salem, B.B., El-Cibahy, A. and El-Raey, M. (1995). Detection of land cover classes in agro-ecosystems of northern Egypt by remote sensing, *International Journal of Remote Sensing* 16, 2581–2594.

Sanz-Cortes, F., Martinez-Calvo, J., Badenes, M.L., Bleiholder, H., Hack, H., Llacer, G. and Meier, U. (2002). Phenological growth stages of olive trees (Olea europaea), *Annals of Applied Biology* 140, 151–157.

Schlenker, W. and Roberts, M.J. (2006). Nonlinear effects of weather on corn yields, *Review of Agricultural Economics* 28, 391–398.

Shivers, S.W., Roberts, D.A. and McFadden, J.P. (2019). Using paired thermal and hyperspectral aerial imagery to quantify land surface temperature variability and assess crop stress within California orchards, *Remote Sensing of Environment* 222, 215–231.

Skees, J.R., Black, J.R. and Barnett, B.J. (1997). Designing and rating an area yield crop insurance contract, *American Journal of Agricultural Economics* 79, 430.

Sklar, A. (1959). Fonctions de Répartition à n Dimensions et Leurs Marges, *Institut Statistique de l'Université de Paris* 8, 229–231.

Smith, V. and Watts, M. (2012). Index based agricultural insurance in developing countries: feasibility, scalability and sustainability. Available from URL: http://citeseerx.ist.psu.edu/viewdoc/download?doi=10.1.1.476.4002&rep=rep1&type=pdf [accessed 15 June 2019].

Spivak, L., Vitkovskaya, I. and Batyrbaeva, M. (2008). Analysis of intra-seasonal variations in the productivity of vegetation in Kazakhstan, using time series remote sensing, *Bulletin of National Academy Science Republic Kazakhstan Series Physics-Mathematics* 4, 29–32.

Turvey, C.G. (2001). Weather derivatives for specific event risks in agriculture, *Review of Agricultural Economics* 23, 333–351.

Turvey, C.G. and Mclaurin, M.K. (2012). Applicability of the normalized difference vegetation index (NDVI) in index-based crop insurance design, *Weather, Climate, and Society* 4, 271–284.

UNESCO (2019). The Olive Grove Landscapes of Andalusia. Available from URL: http://whc.unesco.org/en/tentativelists/6169 [accessed 30 January 2019].

Unganai, L.S. and Kogan, F.N. (1998). Drought Monitoring and corn yield estimation in Southern Africa from AVHRR Data, *Remote Sensing of Environment* 63, 219–232.

United States Geological Survey (2019). Earth explorer-digital elevation. Available from URL: https://earthexplorer.usgs.gov/ [accessed 20 August 2019].

USGS (2020). Mapping, remote sensing, and geospatial data. Available from URL: https://www.usgs.gov/faqs/what-remote-sensing-and-what-it-used?qt-news_science_products=0#qt-news_science_products. [accessed 19 May 2020].

Vedenov, D.V. (2008). Application of Copulas to Estimation of Application of copulas to estimation of joint crop yield distributions. *Contributed Paper at the Annual Meeting of the AAEA,Orlando, USA, July 27–29*.

Vedenov, D.V. and Barnett, B.J. (2004). Efficiency of weather derivatives as primary crop insurance instruments, *Journal of Agricultural Resource Economics* 29, 387–403.

Vroege, W., Dalhaus, T. and Finger, R. (2019). Index insurances for grasslands – A review for Europe and North-America, *Agricultural Systems* 168, 101–111.

Ward, P.S., Makhija, S. and Spielman, D.J. (2020). Drought-tolerant rice, weather index insurance, and comprehensive risk management for smallholders: evidence from a multi-year field experiment in India, *Australian Journal of Agricultural and Resource Economics* 64, 421–454.

Woodard, J. D., Paulson, N. D., Vedenov, D. and Power, G. J. (2011). Impact of copula choice on the modeling of crop yield basis risk, *Agricultural Economics* 42, 101–112.

Wu, W. and De Pauw, E. (2011). A simple algorithm to identify irrigated croplands by remote sensing. *34th International Symposium on Remote Sensing of Environment, At Sydney, Australia*.

Supporting Information

Additional Supporting Information may be found in the online version of this article:

Table S1 Summary statistics of the 16-day indices (satellite indices in percent, precipitation sum index in mm and temperature sum index in °C) for the entire investigation period from 2000 to 2015 and olive oil yields in kg/ha.

Table S2 Spearman correlation coefficients between the VHI values calculated with different *a*-values and the olive oil yield for the studied provinces.

Table S3 Spearman correlation coefficients between the precipitation/temperature values and the VCI values for the non-irrigated/irrigated olive areas for the whole investigation period and the studied provinces.

Figure S1 Main phenological stages of olive tree vegetation.

Figure S2 Digital elevation model of the 5 investigated provinces of Andalusia.